Chapter IV

GEOCHRONOLOGY OF THE JEQUIÉ-ITABUNA GRANULITIC BELT AND OF THE CONTENDAS-MIRANTE VOLCANO-SEDIMENTARY BELT

MOACYR M.MARINHO[1]; PHILLIPHE VIDAL[2]; CHANTAL ALIBERT[3]; JOHILDO S.F.BARBOSA[4] and PIERRE SABATÉ[4,5]

[1]CBPM - Companhia Baiana de Pesquisa Mineral, 4ª Av., 460, CAB, 41206, Salvador, Bahia, Brazil
[2]Department de Sciences de la Terre, Université Blaise Pascal - 5, Rue Kessler, 63038, Clermont Ferrand, France
[3]CPRG, BP 20, 54501 Vandoeuve, France.
[4]Curso de Pós-Graduação em Geologia, PPPG - Programa de Pesquisa e Pós-Graduação em Geofísica, Instituto de Geociências, Universidade Federal da Bahia, Rua Caetano Moura, 123, Federação, 40210-350, Salvador, Bahia, Brazil
[5]ORSTOM, C. Postal 4741, Shopping Barra, 40149-900 Salvador, Bahia, Brazil

INTRODUCTION

Almost all geochronologic data available until 1985 for the Jequié-Itabuna granulitic belt and for the Contendas-Mirante volcano-sedimentary belt were based on whole rock Rb-Sr systems for which the cogeneticity of the samples used to calculate the isochronic ages were generally not assured. Thus, in spite of the enormous contribution which the several studies developed until then (Cordani, 1973; Marinho et al., 1978; Cordani & Iyer, 1979; Marinho et al., 1979, 1980; Marinho & Sabaté, 1982; Cordani et al., 1985; Delhal & Demaiffe, 1985; Mascarenhas & Garcia, 1989) have brought to the definition of the main geotectonic cycles of the São Francisco Craton, they were not successful in clearly defining specific geological events in those regions.

The studies carried out by Barbosa (1986) are a milestone in the understanding of the magmatic-metamorphic evolution of the Jequié-Itabuna granulitic belt. They allowed geochronologic reappraisals of the belt through the Rb-Sr, Sm-Nd, Pb-Pb methods (Wilson, 1987; Marinho, 1991) as well as, in a smaller scale so far, through the U-Th-Pb ion microprobe zircon method (Alibert & Barbosa, 1992).

With regard to the Contendas-Mirante volcano-sedimentary belt, including the basement domes and its intrusive bodies, multidisciplinary investigations (petrography, geochemistry, metamorphism and geochronology) performed by Marinho (1991) allowed the reappraisal of the existing geochronological data within the regional geologic evolution context. The isotopic determinations made by Marinho (1991) involved the Rb-Sr, Sm-Nd and Pb-Pb methods as well as one age determination by U-Pb in zircon, by the conventional method. Other relevant contributions include: (i) the data obtained by Martin et al. (1991) on the Sete Voltas Archean dome, obtained by the Rb-Sr method and single grain evaporation of zircons (3 samples); (ii) the U-Th-Pb ion microprobe zircon determinations made by Nutman & Cordani (chapter V), working on samples collected by Marinho et al. (1980) from the Boa Vista/Mata Verde, Sete Voltas, Lagoa do Morro and Serra dos Pombos Archean domes; and (iii) the determinations by Nutman, Cordani and Sabaté (in press) on one conglomerate sample from the Areião Formation (upper unit of the volcano-sedimentary sequence).

The lack of higher resolution geochronological data as, for example, those produced by the different mono-zircon techniques, imposes restrictions to a finer-scale ordering of the regional geological events. Furthermore, despite the progress in the petrologic understanding of the region, difficulties still persist as to the identification of local heterogeneities, which, in turn, leads to uncertainty involving the cogenetic relations between samples used in the linear regressions and, as a result, the real meaning of the age data obtained.

THE JEQUIÉ-ITABUNA GRANULITIC BELT

This granulitic belt is divided here into the "Jequié-Mutuípe-Maracás Domain" and the "Atlantic Coast Domain".

JEQUIÉ-MUTUÍPE-MARACÁS DOMAIN

This domain comprises "*Plutonic Rocks equilibrated in Granulite Facies*" and "*Ortho- and Paraderived Rocks Metamorphosed in Granulite Facies*".

Plutonic rocks equilibrated in granulite facies

These include the charno-enderbitic rocks from the Laje-Mutuípe region and the charnockitic rocks from the Maracás region.

Charno-enderbitic rocks from the Laje-Mutuípe region

Until late 1991 it was accepted that the geochronological evolution of this region followed the model proposed by Wilson (1987). This model was based on the following data,

originated from a sampling supported on Barbosa's (1986) work, that considered the plutonic rocks of this region as cogenetic:

. Rb-Sr errorchron (Fig. IV.1) of fifteen samples (age = 2932±124 Ma; Sr_i = 0.7020; MSWD = 42); and

. T_{DM}Nd model ages between 2920 and 3150 Ma (Table IV.1).

In his model, Wilson considered 3.0 Ga as the probable age of formation of these rocks from the mantle, which would agree with the $\epsilon Nd_{(3000\ Ma)}$ values, generally above +1.8 (Table VI.1). The Pb-Pb diagram shown in the Fig. IV.2, which suggested an age of 3420 Ma (MSWD = 1.6), was interpreted within a three-stage model where the alignment obtained would represent a retarded paleo-isochron.

U-Th-Pb zircon ion-microprobe work by Alibert & Barbosa (1992) in enderbites from Mutuípe and in charnockites from Jequiriçá resulted in ages of 2689±1 Ma and 2810 Ma, respectively (Fig. IV.3). These ages, which have been assumed as representative of the intrusion time of those rocks, indicate heterogeneity in the charno-enderbitic domain from the Laje-Mutuípe region, which is also stressed by the geochemical study presented in chapter II. The comparison of these ages with the T_{DM}Nd model ages revals a certain time of crustal residence for the protoliths of the charno-enderbitic rocks. This crustal residence is also indicated by the $Nd_{(2700\text{-}2800\ Ma)}$ values between +0.5 and -3.7.

Charnockitic Rocks from The Maracás Region

The following data have been presented by Marinho (1991) for these charnockitic rocks:

. Rb-Sr data scattered between 2800 and 2300 Ma on the $^{87}Sr/^{86}Sr$ vs $^{87}Rb/^{86}Sr$ diagram (Fig. IV.4);

. Pb-Pb isochron (Fig. IV.5) of eleven samples (age = 2660±76 Ma; μ_1 = 8.58; MSWD = 1.80);

. T_{DM}Nd model ages between 3180 and 3390 Ma and $\epsilon Nd_{(2700\ Ma)}$ between -3.0 and -4.9 (Table IV.1).

The position of the Pb-Pb isochron above the normal evolution curve for the terrestrial lead (Fig. IV.5) indicates an isotopic evolution in at least three stages. This evolution is in agreement with the crustal origin denoted by the negative values of $\epsilon Nd_{(2700\ Ma)}$.

The point scattering on the diagram of Fig. IV.4 shows that the Rb-Sr system was disturbed by some partial loss or gain of Rb, probably related to retrograde transformations of this western part of the "Jequié-Mutuípe-Maracás Domain".

Although revealing a polyphase history, this data set do not allow the determination of the intrusive age of these charnockitic rocks in the Maracás region. It is believed that the zircon U-Pb method may solve this problem.

Ortho- and paraderived rocks metamorphosed in granulite facies

Most of the data on these rocks comes from Wilson (1987). They were obtained from rocks collected at the Jequié quarry and from homogeneous rocks collected at the western outskirts of the Jequiriçá town.

Banded quartzo-feldspathic rocks with mafic intercalations predominate in the Jequié quarry (stop 8-1). Gray, lighter lithologies truncate the banding and, in turn, are clearly truncated by pegmatoid viens. The whole assemblage is metamorphosed in granulite facies. According to Wilson's descriptions, the sampling emcompassed the newly formed lithologies, but their distinction into two different types is not mentioned. The data presented are as follows:

. Rb-Sr errochron (Fig. IV.6) of six samples (age = 2085±222 Ma; Sr_i = 0.7297; MSWD = 11);

. Pb-Pb isochron (Fig. IV.7) of twelve

Table IV.1 - Sm-Nd data for the Jequié-Itabuna granulitic belt.

UNIT	SAMPLE	Sm(ppm)	Nd(ppm)	147Sm/144Nd	143Nd/144Nd	ENd(o)	ENd(t)	Tchur(Ga)	TDm(Ga)	ENd(o)Dm	t(AE)	Lithology	Locality	
1	1263 PJ R12(2)	13.87	90.86	0.0923	0.511094	-30.1		2.244	2.488	8.75		shoshonite	Ipiaú road - BR 101	
	CJ21	4.12	31.5	0.0791	0.510900	-33.9		2.243	2.464	8.75		felsic granulite	Ituberá-Gandu road	
(*)	CJ33	1.48	5.01	0.1800	0.512066	-11.2				8.75		mafic granulite	Ubaitaba-Maraú road	
(*)	CJ34A	0.56	4.74	0.0724	0.510370	-44.2		2.765	2.912	8.75		felsic granulite	Ubaitaba-Maraú road	
(*)	CJ34B	2.29	7.35	0.1890	0.512599	-0.8				8.75		mafic granulite	Ubaitaba-Maraú road	A
(*)	CJ19	3.31	14.55	0.1380	0.511653	-19.2		2.544	2.869	8.75		mafic granulite	Ituberá-Gandu road	
(*)	CJ11	4.57	23.80	0.1170	0.511403	-24.1		2.351	2.639	8.75		felsic granulite	Maricoabo	
(*)	CJ13	20.00	150.00	0.0813	0.510965	-32.6		2.201	2.431	8.75		shoshonite	Cajaíba	
2(**)	1	1.9	10.5	0.1119	0.511042	-31.1	-1.92	2.851	3.041	8.75	2.700			
(**)	4	9.0	60.7	0.0900	0.510635	-39.1	-2.31	2.844	3.001	8.75	2.700			
(**)	6	12.1	65.9	0.1109	0.511032	-31.3	-1.77	2.836	3.026	8.75	2.700			
(**)	10	6.7	36.0	0.1116	0.511049	-30.9	-1.68	2.829	3.021	8.75	2.700			
(**)	13	1.8	10.5	0.1061	0.510847	-34.9	-3.7	2.993	3.150	8.75	2.700			
(**)	14	11.8	61.9	0.1157	0.511091	-30.2	-2.27	2.893	3.082	8.75	2.700			
(**)	21	15.7	88.9	0.1066	0.511021	-31.5	-0.5	2.720	2.921	8.75	2.700			
(**)	23A	10.7	63.6	0.1015	0.510920	-33.5	-0.71	2.735	2.924	8.75	2.700			
3(***)	MM-138	29.69	137.93	0.1301	0.511211	-27.8	-4.91	3.244	3.394	8.75	2.700			
(***)	MM-140A	15.43	69.97	0.1333	0.511382	-24.5	-2.67	3.001	3.209	8.75	2.700			B
(***)	MM-170	19.06	92.87	0.1241	0.511163	-28.8	-3.76	3.075	3.247	8.75	2.700			
(***)	MM-137	21.76	106.2	0.1239	0.511198	-28.1	-3.01	2.994	3.182	8.75	2.700			
4(**)	17A	7.0	56.0	0.0756	0.510714	-37.5		2.410	2.605	8.75		felsic granulite	Jequié quarry	
(**)	17D	4.2	28.9	0.0886	0.510680	-38.2		2.745	2.914	8.75		felsic granulite	Jequié quarry	
	1263 PJ R09	9.53	47.28	0.1219	0.511082	-30.3		3.147	3.302	8.75		mafic horizon	Jequié quarry	
	1263 PJ R10	4.33	17.6	0.1487	0.511586	-20.5				8.75		mafic horizon	Jitauna	
	1263 PJR11	3.72	12.24	0.1838	0.512461	-3.5				8.75		mafic horizon	Ipiaú	
(**)	16B	12.3	63.6	0.1079	0.510878	-34.3		3.001	3.159	8.75		felsic granulite	Eng° França	
	1263 PJ R04	5.03	22.4	0.1356	0.511386	-24.4		3.104	3.295	8.75		mafic boudin	Eng° França	
	1263 PJ R05(6)	4.8	28.57	0.1016	0.510733	-37.2		3.034	3.178	8.75		S granite	Sta. Inês-Cravolândia road	
	CJ27	3.52	13.34	0.1594	0.511935	-13.7				8.75		mafic horizon	Gandu quarry	
	CJ29	0.79	5.21	0.0912	0.510946	-33.1		2.432	2.648	8.75		pegmatoid rock	Gandu quarry	

A-Atlantic coast Domain
Jequié-Mutuípe-Maracás Domain

1-Granulites from Atlantic coast Domain
2-Charno-enderbitic rocks from Lage-Mutuípe region
3-Charnockitic rocks from Maracás region
4-Supracrustal rocks metamorphosed in granulite facies

(*) Barbosa (1990)
(**) Wilson 1987
(***) Marinho (1991)

Bol.IG-USP, Publ.Especial, 15:73-96, 1993.

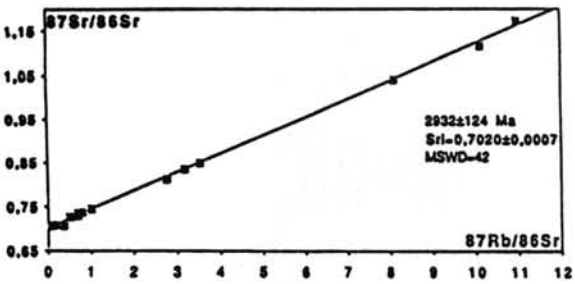

Figure IV.1 - Rb-Sr (whole rock) diagram for charno-enderbitic rocks from the Lage-Mutuípe region (Wilson, 1987).

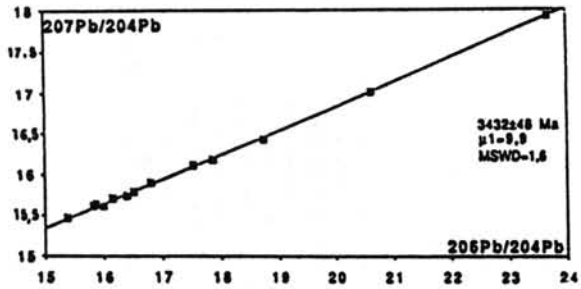

Figure IV.2 - $^{207}Pb/^{204}Pb$ vs. $^{206}Pb/^{204}Pb$ (whole rock) diagram for charno-enderbitic rocks from the Lage-Mutuípe region (Wilson, 1987).

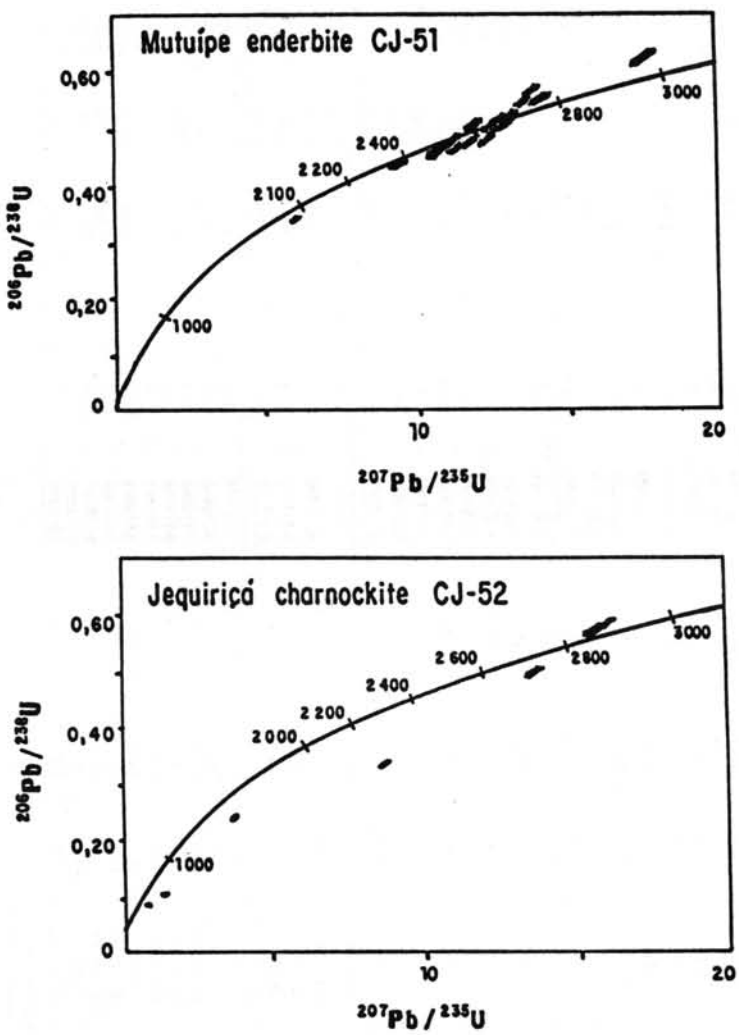

Figure IV.3 - U-Pb concordia diagram, Mutuípe enderbite CJ-51 and Jequiriçá charnockite CJ-52 (Alibert & Barbosa, 1992).

samples (age = 1970±136 Ma; μ_1 = 8.4; MSWD = 0.74);

. T_{DM}Nd model ages of two samples with values of 2900 and 2600 Ma.

The homogeneous rocks from west of Jequiriçá were interpreted by Barbosa (1986, 1990) as originated during granulite metamorphism, through the anatexis of supracrustal lithologies, although now (chapter II) they are considered as orthoderived rocks. Wilson's isotopic data for them are the following:

. Rb-Sr isochron (Fig. IV.8) of four samples (age = 2699±24 Ma; Sr_i = 0.7194; MSWD = 1.7);

. T_{DM}Nd model age of one sample with value of 3160 Ma.

In addition to Wilson's data, some Sm-Nd determinations have recently been made on these rocks by Alibert, Barbosa, Marinho and Vidal (in prep.), producing T_{DM}Nd model ages between 3150 and 3300 Ma, except for one with 2650 Ma for a pegmatoid vein from the Gandu quarry (Table IV.1)

On the basis of this set of isotopic data, the following considerations can be made about the granulite facies ortho- and paraderived rocks of the "Jequié-Mutuípe-Maracás Domain":

. This lithologic assemblage was submitted to granulitic metamorphism of Transamazonian age (ca 2.0 Ga);

. If the origin proposed by Barbosa (1986, 1990) for the homogeneous rocks from west of Jequiriçá involving anatexis associated to granulitic metamorphism, is correct, this metamorphism is older (ca 2.7 Ga);

. The T_{DM}Nd model ages of about 2.6 Ga obtained in quartzo-feldspathic veins of Jequié and Gandu quarries may indicate the presence in the area of material of shorter crustal residence time in relation to the other lithologies. However, such values could also have no geological meaning, reflecting only a decrease in the Sm/Nd ratio due to fractionation of LREE within the crust. Similar phenomenon was described by Pimentel & Charnley (1991) for evolved granitic rocks from Central Brazil.

ATLANTIC COAST DOMAIN

Most of the available geochronological data for this domain (Mascarenhas & Garcia, 1989) are related to the Rb-Sr system. The lack of petrologic control for the analyzed rocks precludes the interpretation of the geological significance of the ages between 2.0 and 2.3 Ga obtained in the several linear regressions.

Sm-Nd determinations (Table IV.1) made at the University of Clermont-Ferrand II, France (Barbosa 1990) and others still unpublished (Alibert, Barbosa, Marinho and Vidal, in prep. - Table IV.1) in granulite facies mafic and felsic magmatic lithologies give T_{DM}Nd model ages between 2.4 and 2.9 Ga. The available data suggest crustal accretion at about 2.4 Ga followed by granulitic metamorphism during the Early Proterozoic in the "Atlantic Coast Domain".

THE CONTENDAS-MIRANTE VOLCANO-SEDIMENTARY BELT

As discussed previously (Chapter II), the following domains are identified within the Contendas-Mirante volcano-sedimentary belt:

. The basement domes;

. The volcano-sedimentary sequence; and

. The intrusive rocks.

THE BASEMENT DOMES

This is the domain of the ancient gray gneisses (ca. 3.4 Ga), similar to the TTG

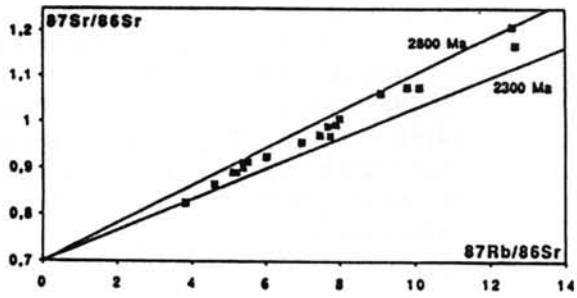

Figure IV.4 - Rb-Sr (whole rock) diagram for charnockites from the Maracás region (Marinho, 1991).

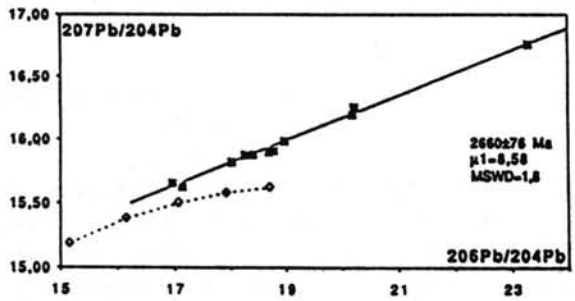

Figure IV.5 - $^{207}Pb/^{204}Pb$ vs. $^{206}Pb/^{204}Pb$ (whole rock) diagram for charnockites from the Maracás region (Marinho, 1991).

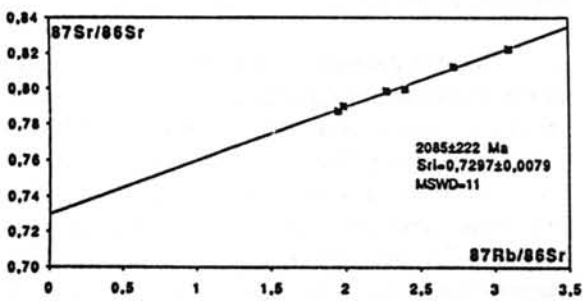

Figure IV.6 - Rb-Sr (whole rock) diagram for newly-formed quartz-feldspathic rocks from the Jequié quarry (Wilson, 1987).

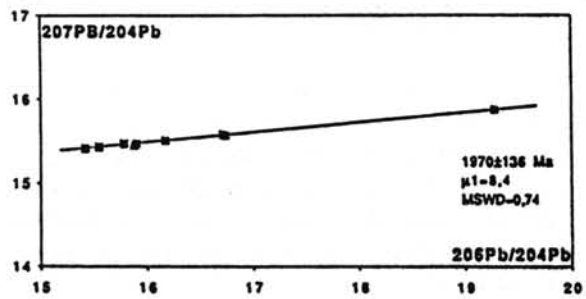

Figure IV.7 - $^{207}Pb/^{204}Pb$ vs. $^{206}Pb/^{204}Pb$ (whole rock) diagram for mewly-formed quartz-feldspathic rocks from the Jequié quarry (Wilson, 1987).

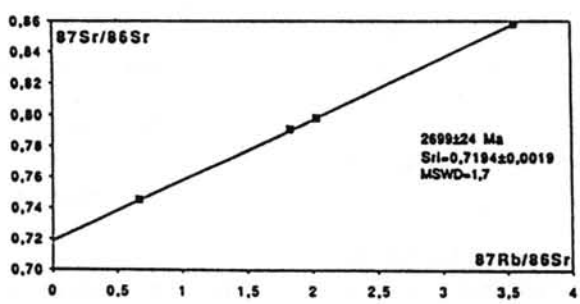

Figure IV.8 - Rb-Sr (whole rock) diagram for the homogeneous rocks from W of Jequiriçá town (Wilson, 1987).

(tonalite-trondhjemite-granodiorite) terrains. Among the different massifs that crop out in the SE sector of the volcano-sedimentary belt, those of Sete Voltas and Boa Vista/Mata Verde have geochronological data available. The first references to radiometric dates on these rocks were made by Marinho et al. (1978, 1979, 1980) with Rb/Sr isochronic ages of ca 3.4 and 3.1 Ga for the Sete Voltas and the Boa Vista/Mata Verde massifs, respectively.

Sete Voltas Massif

As discussed in Chapter II, the work of Martin et al. (1991) allowed the identification of *enclaves of old gray gneisses* (ca 3.4 Ga) within *young gray gneisses* (ca 3.15 Ga) and *porphyritic granitoids* (ca 3.25 Ga) that are cutted by *gray granite veins*. The radiometric data obtained are the following (Fig. IV.9):

Lithology	Isochron Age (Rb-Sr)	Sr_i	Single Grain Evaporation of Zircon Age
old gray gneisses	3420±90 Ma	0.6997±0.0004	3394±5 Ma
young gray gneisses	3140±90 Ma	0.7017±0.0008	3158±2 Ma
porphyritic granodiorites	3170±160 Ma	0.7014±0.0011	3243±5 Ma

The initial Sr ratio (Sr_i) suggests that the old gray gneisses were mostly of juvenile origin with few or no crustal contamination. On the other hand, the Sr_i of both young gray gneisses and porphyritic granodiorites are in the higher range of mantle values for that period. This could be caused by crustal recycling. In these conditions the contaminant could be the old gray gneisses.

Concordant ages of 3403±5 Ma determined by Nutman & Cordani (chapter V, in press) using SHRIMP in zircons from the Sete Voltas massif tonalite confirm the data previously obtained by Martin et al. (1991) on that same tonalite. However, a concordant age of 3473+8 Ma determined by Nutman & Cordani (op. cit.) in a round structural core of a grain that presents a second zircon overgrowth suggests the existence of older rocks.

Boa Vista/Mata Verde Massif

The Rb-Sr (Table IV.2) and Pb-Pb (Table IV.3) available data have been re-evaluated by Wilson (1987) who carried out a complementary sampling and combined study of those methods with Sm-Nd, after geochemical work to investigate cogeneticity. The results are the following:

. Rb-Sr errorchron (Fig. IV.10) of nine samples (age = 3444±209 Ma; Sr_i = 0.7008±0.0015; MSWD = 21). Four samples were eliminated from the regression (37, 38, AC1c and AC1d). The data determined by Marinho (1991) is plotted in the diagram (Fig. IV.10) as filled lozenges;

. Pb-Pb errorchron (Fig. IV.11) of twelve samples (age = 3381±83 Ma; μ_1 = 8.7; MSWD = 8.7). Two samples were eliminated from the regression; and

. T_{DM}Nd model ages (Table IV.4) between 3450 and 3530 Ma, except for sample 38 which gives an age of 3185 Ma. The Nd(3350 Ma) of this sample is +3.6 whereas for the others it ranges between -0.8 and -2.1 (Table IV.4).

Although the isochrons are of low quality, the values obtained suggest an ancient age for the massif, as it had already been pointed out by Marinho et al. (1980) and Cordani et al. (1985). The observed dispersion reflects essentially a partial resetting of the Rb-Sr and Pb-Pb systems and, to a lesser extent, the heterogeneity of the Boa Vista/Mata Verde massif. Such a heterogeneity has been shown by Marinho (1991), who identified a more potassic facies of granitic composition (samples 196, 202, 204B, AC1c and AC1b) and of limited occurence within the essentially tonalitic lithologies of the massif.

The definitive confirmation of the massif

Table IV.2 - Rb-Sr data.

SAMPLE	Rb(ppm)	Sr(ppm)	87Rb/86Sr	87Sr/86Sr
CHARNO-ENDERBITIC ROCKS FROM LAGE - MUTUIPE REGION				
1	43	668	0.1863	0.70900
2	32	670	0.1380	0.70779
3	55	307	0.5154	0.72686
4	70	288	0.7047	0.73527
5	83	336	0.7119	0.73039
6	84	240	1.0230	0.74493
9	93	333	0.8081	0.73713
10	256	76	10.1399	1.11496
11	145	133	3.1872	0.83464
12	188	52	10.9915	1.17276
13	79	375	0.6077	0.72846
18	29	813	0.1039	0.70672
19A	65	496	0.3755	0.70680
20	195	205	2.7759	0.81133
21	193	160	3.5410	0.84905
22	296	109	8.1169	1.04045
14	377	67	17.3773	1.37384
23A	406	86	14.4929	1.27870
23B	370	41	29.0054	1.83550
CHARNOCKITIC ROCKS FROM MARACAS REGION				
MM-134	174.3	69.3	7.4646	0.97159
MM-137	125.7	71.2	5.1987	0.88984
MM-138	130.5	83.3	4.6018	0.86404
MM-139	135.5	78.1	5.1090	0.89007
MM-140A	98.5	75.6	3.8123	0.82385
MM-141	161.8	38.6	12.6724	1.16721
MM-143	181.1	68.3	7.8866	0.99455
MM-166	176.5	67.7	7.7368	0.97075
MM-167	146,0	80,0	5.3794	0.90009
MM-170	142.4	78.2	5.3725	0.90981
MM-177	143.4	76.8	5.5105	0.91284
MM-178	185.5	61,0	9.1039	1.06307
MM-180	199.2	59,0	10.1197	1.07566
MM-194	175.5	65.5	7.9792	1.00739
MM-218	189,0	57.8	9.8013	1.07615
MM-219	174.4	67.5	7.682	0.99073
MM-222	157.1	77.1	6.0196	0.92355
MM-217	218.7	52.7	12.5962	1.20988
MM-223	170.8	72.5	6.9811	0.95552
HOMOGENEOUS ROCKS FROM W OF JEQUIRIÇA TOWN				
16B	129	185	2.0366	0.79857
16C	110	175	1.8324	0.79146
16D	55	238	0.6708	0.74550
16E	160	132	3.5654	0.85826
16 F	114	220	1.5063	0.76970
16G	98	231	1.2330	0.76083
NEWLY-FORMED ROCKS FROM THE JEQUIE QUARRY				
17A	146	138	3.0966	0.82253
17C	158	202	2.2736	0.79871
17D	94	138	1.9848	0.79027
17 F	108	161	1.9500	0.78758
17B	171	182	2.7251	0.81261
			2.4000	0.80000
17E	106	168	1.8355	0.78126
BARRA DA ESTIVA ROAD JUNCTION SUB-VOLCANIC BODY				
42A	62	63	2.8761	0.83225
42B	52	69	2.1915	0.81461
42C	55	62	2.5752	0.82309
42D	53	67	2.3392	0.81771
42E	46	65	2.0543	0.80718
42 F	35	60	1.6752	0.79832
42G	51	59	2.544	0.82401
42I	68	75	2.6423	0.8295
42J	68	76	2.6313	0.82902
CM-20	51.2	66	2.27	0.8161
CM-23	51.5	56	2.69	0.8281
CM-26	54.2	58.4	2.72	0.8311
CM-29	54.5	70.9	2.17	0.8112
SM-3-16C	59.8	58.8	2.98	0.8368
SM-3-16F	46.9	74.6	1.84	0.8022
SM-3-16G	56.5	75.2	2.19	0.8094
41	49	73	1.9678	0.79765
SM-3-16A	61.9	44.9	4.06	0.8793
SM-3-16D	70.2	72.8	2.83	0.838

SAMPLE	Rb(ppm)	Sr(ppm)	87Rb/86Sr	87Sr/86Sr
NEOSOMES WITHIN METAPELITES (MIDDLE UNIT)				
MM-200A	100.3	284.1	1.0239	0.73271
MM-200B	32.1	312.9	0.2969	0.71170
MM-205A	57.6	230.1	0.7253	0.72327
MM-205B	75.7	278.2	0.7887	0.72621
MM-205C	77.9	231.7	0.9750	0.73154
MM-205D	66.5	258.8	0.7462	0.72494
MM-205F	71.8	255	0.8161	0.72673
MM-205H	51.7	250	0.5991	0.72091
MM-206B	238.8	344	2.0019	0.76052
BOA VISTA/MATA VERDE GRANITOID				
MM-196	107.5	124.9	2.5204	0.83222
MM-202	145.5	118.7	3.6082	0.88590
MM-204B	128.1	147.9	2.5336	0.82111
MM-197	48.7	181.7	0.7784	0.74623
MM-198	51,0	363.7	0.4061	0.71885
MM-199	53.7	62.4	0.4292	0.71968
MM-201	79.2	411.6	0.5577	0.72635
MM-204A	60.3	181,0	0.9687	0.75911
31	58	373	0.4512	0.72390
32	62	330	0.5457	0.73021
33	68	372	0.5316	0.72721
35	40	415	0.2823	0.71532
36	54	360	0.4351	0.72084
37	76	206	1.0737	0.76328
38	83	171	1.4195	0.78411
AC1B	137.3	152.2	2.64	0,8310
AC1C	139.2	163,0	2.5	0.8230
AC1E	105.2	240.7	1.27	0.7658
AC1I	54.4	441.9	0.36	0.7184
AC1Ad	78,0	215.2	1.05	0.7643
AC1Ac	93.1	209.5	1.29	0.7718
LAGOA DO MORRO GRANITOID				
MM-209A	126.8	369.5	0.9963	0.74347
MM-209B	123.6	372.4	0.9636	0.74388
MM-209C	122.3	391.3	0.9074	0.74281
MM-210A	165.7	257.9	1.8724	0.78246
MM-210B	144.5	261.5	1.6083	0.76909
MM-211A	144.4	292.3	1.4372	0.76428
MM-211B	147.7	268.5	1.6011	0.76906
SERRA DOS POMBOS GRANITOID				
MM-212A	144,0	131.6	3.2094	0.84848
MM-212B	142.1	149,0	2.7953	0.84160
PE DE SERRA GRANITE				
MM-30A	127.4	101.7	3.6679	0.83086
MM-30C	155.3	100.9	4.5145	0.84885
MM-30E	108.3	124.4	2.5413	0.79952
MM-32A	107.8	118.1	2.6662	0.80602
MM-32B	148,0	60.2	7.2941	0.96843
MM-60A	193.9	64.6	8.9537	1.02525
MM-160B	133.3	107.8	3.6220	0.83489
MM-160C	156.9	123.6	3.7176	0.83291
MM-31	133.6	125.5	3.1117	0.81324
RT-11219	142.6	122.6	3.4060	0,00000
MM-132	62.7	119.3	1.5300	0.77116
MM-163	130,0	54.3	7,0351	0.88788
SM318A	61.15	122.7	1.46	0.7713
SM318C	19.6	93.3	0.61	0.7549
TRANSAMAZONIAN GRANITE (GAMELEIRA)				
MM-91A	270.5	146.3	5.4292	0.86052
MM-92	224.8	171.7	3.8276	0.81478
MM-95	282.1	161.3	5.1289	0.84709
MM-96	258.8	94.2	8.1241	0.93353
MM-97B	276.4	145.5	5.5819	0.86737
MM-101	274.7	113.9	7.1141	0.90776
RT11218	341.5	148.2	6.7900	0.89570
TRANSAMAZONIAN GRANITE (RIACHO DAS PEDRAS)				
MM-99B	200	14.5	44.6843	1.96824
MM-99C	215	14.4	49.0709	2.08941
MM-99D	220	13.2	55.6716	2.26353
MM-99F	214	15.5	44.8928	2.011
MM-99H	279	6.01	208.8250	6.40609
MM-99I	135	14.4	29.3074	1.54446
MM-99J	333	5.3	360.5014	10.6001
MM-99K	308	5.4	297.9953	9.02467
MM-99M	327	4.8	417.8310	12.2267

Table IV.3 - Pb-Pb data.

SAMPLE	206Pb/Pb204	207Pb/204Pb	208Pb/204Pb	t (Ga)	TH/U
CHARNO-ENDERBITIC ROCKS FROM LAGE-MUTUIPE REGION					
1	15.826	15.612	35.214	3.0	3.2
2	15.881	15.636	35.097	3.0	3.0
4	16.155	15.705	40.683	3.0	9.1
5	15.387	15.466	36.191	3.0	5.2
6	16.001	15.612	35.714	3.0	3.6
9	16.808	15.898	36.627	3.0	3.7
13	17.53	16.106	36.05	3.0	2.7
14	20.618	17.013	40.096	3.0	3.5
18	16.404	15.736	36.541	3.0	4.1
19A	17.863	16.176	35.544	3.0	2.1
20	16.516	15.786	35.908	3.0	3.3
22	18.735	16.426	37.35	3.0	2.9
23A	23.682	17.925	44.823	3.0	4.2
3	17.495	15.98	42.316	3.0	7.8
10	17.929	16.084	38.919	3.0	4.6
11	17.772	15.958	40.678	3.0	6.1
12	17.448	15.961	37.856	3.0	4.2
21	19.424	16.431	42.46	3.0	5.5
23B	23.341	17.41	51.104	3.0	6.5
CHARNOCKITIC ROCKS FROM MARACAS REGION					
MM-137	16.968	15.654	41.453	2.7	8.8
MM-138	18.775	15.91	44.49	2.7	7.9
MM-140A	17.139	15.627	36.72	2.7	3.5
MM-141	18.402	15.877	40.177	2.7	5.2
MM-170	18.018	15.819	40.881	2.7	6.2
MM-180	20.184	16.201	41.299	2.7	4.4
MM-194	18.969	15.987	42.674	2.7	6.4
MM-217	23.294	16.757	43.138	2.7	3.7
MM-218	20.215	16.259	42.91	2.7	5.3
MM-222	18.69	15.899	40.527	2.7	5.2
MM-223	18.257	15.873	39.464	2.7	4.8
BARRA DA ESTIVA ROAD JUNCTION SUB-VOLCANIC BODY					
41	28.348	18.305	49.813	3.0	4.1
42A	26.553	18.078	47.749	3.0	4.1
42B	31.355	19.058	53.293	3.0	4.1
42C	26.266	17.755	47.575	3.0	4.1
42D	32.66	19.32	55.037	3.0	4.2
42E	34.903	19.816	57.16	3.0	4.1
42	34.315	19.618	55.95	3.0	4.0
42G	32.389	19.532	54.469	3.0	4.1
42H	27.587	18.261	49.172	3.0	4.2
42I	29.033	18.602	50.936	3.0	4.2
42J	28.678	18.472	50.699	3.0	4.2
THOLEIITIC VOLCANIC ROCKS (LOWER UNIT)					
MM-7	20.856	16.028	40.749	3.0	3.7
MM-8	20.907	16.122	41.017	3.0	3.8
MM-8bis	20.466	16.005	40.167	3.0	3.7
MM-9	20.33	16.012	40.056	3.0	3.7
MM-11	20.811	16.001	41.158	3.0	4.0
MM-6A	17.149	15.353	38.224	3.0	4.8
MM-6B	17.135	15.505	37.435	3.0	4.1
MM-15	17.558	15.641	37.103	3.0	3.5
MM-17	16.693	15.233	37.998	3.0	5.2
MM-20	19.452	15.939	38.63	3.0	3.3
MM-21	18.206	15.77	37.494	3.0	3.3
MM-22A	18.417	15.826	37.42	3.0	3.2
MM-22C	18.336	15.807	37.425	3.0	3.2
MM-23	17.602	15.474	37.577	3.0	3.8
MM-40	16.43	15.597	35.883	3.0	3.3
BANDED IRON PORMATIONS (LOWER UNIT)					
MM-213A	16.686	15.643	35.82	3.0	3.0
MM-213Bm	16.723	15.682	36.705	3.0	3.9
MM-213Br	16.897	15.717	37.057	3.0	4.0
MM-213Ba	16.943	15.72	37.094	3.0	4.0
MM-231C	15.067	15.166	34.517	3.0	3.1
MM-213Cp	15.488	15.312	35.129	3.0	3.5
MM-213D	14.891	15.223	34.571	3.0	3.5
MM-213E	14.696	15.135	34.358	3.0	3.4
MM-230A	15.626	15.46	35.047	3.0	3.2
MM-230B	15.665	15.472	35.178	3.0	3.3
MM-230E	16.794	15.719	35.947	3.0	3.1
MM-215A	21.732	16.07	38.914	3.0	2.6
MM-215C	15.488	15.572	34.835	3.0	3.0
MM-215Cbis	17.766	15.65	37.457	3.0	3.6
MM-230C	15.39	15.578	34.771	3.0	3.1
MM-230D	15.385	15.553	34.77	3.0	3.1

SAMPLE	206Pb/Pb204	207Pb/204Pb	208Pb/204Pb	t (Ga)	TH/U
CALCO-ALKALINE VOLCANIC ROCKS (MIDDLE UNIT)					
MM-25A	30.639	18.017	46.826	2.5	2.8
MM-27	28.898	17.7	45.072	2.5	2.7
MM-28B	24.504	17.007	41.549	2.5	2.7
MM-24	38.666	19.037	53.03	2.5	2.8
MM-39	25.904	19.933	42.023	2.5	2.5
MM-98	19.619	15.934	39.437	2.5	3.7
MM-151B	19.211	15.869	39.056	2.5	3.7
MM-151C	19.562	15.897	40.485	2.5	4.4
MM-152C	21.562	16.242	42.816	2.5	4.4
MM-158B	41.712	19.6	54.858	2.5	2.77
RIO JACARE SILL					
MM-159A	25.027	16.878	43.309	2.5	3.1
MM-159B	16.624	15.511	35.677	2.5	27,0
MM-159C	19.912	16.036	39.087	2.5	3.3
MM-159D	18.166	15.72	37.239	2.5	3.1
MM-227A	21.049	16.24	42.167	2.5	4.3
MM-227B	16.26	15.431	35.607	2.5	3.0
MM-35	16.171	15.456	35.733	2.5	3.4
MM-37	18.423	15.855	37.737	2.5	3.3
MM-224A	16.417	15.512	35.584	2.5	2.8
MM-224C	15.956	15.397	35.44	2.5	3.2
MM-224D	18.923	15.982	37.095	2.5	2.5
MM-228	16.74	15.594	36.405	2.5	3.6
BOA VISTA/MATA VERDE GRANITOID					
31	18.429	15.795	43.558	3.35	6.9
32	16.823	15.545	40.556	3.35	6.8
33	15.695	15.148	42.622	3.35	11.1
34	16.411	15.356	42.303	3.35	9.0
35	14.698	14.968	40.808	3.35	12.6
36	15.793	15.19	41.981	3.35	10.1
37	16.891	15.97	45.589	3.35	10.6
38	16.68	15.398	48.151	3.35	13.2
AC-1H	21.53	16.85	48.89	3.35	6.7
AC-1I-1	15.33	15.03	42.92	3.35	12.6
AC-1I-2	15.06	14.96	42.44	3.35	13.2
AC-1B	15.31	15.11	44.32	3.35	14.4
AC-1C	15.32	15.11	44.82	3.35	14.9
AC-1E	15.18	15.03	49.24	3.35	20.9
NEWLY-FORMED ROCKS FROM THE JEQUIE QUARRY					
17A	19.281	15.876	49.265		
17B	16.719	15.577	40.959		
17C	15.785	15.468	39.361		
17D	16.742	15.571	44.288		
17 F	15.904	15.467	40.537		
17G	16.174	15.507	42.411		
17E	17.454	15.746	41.593		
LAGOA DO MORRO GRANITOID					
MM-209B	18.291	16.026	40.857	3.2	5.5
MM-210A	16.973	15.325	45.726	3.2	11.1
MM-209A	18.269	15.82	41.495	3.2	5.9
MM-209Abis	18.271	15.833	41.59	3.2	6.0
MM-209C	18.938	15.91	41.547	3.2	5.3
MM-210B	19.45	15.916	42.541	3.2	5.5
MM-211A	20.467	16.265	42.833	3.2	4.9
MM-211Abis	20.512	16.311	43.002	3.2	5.0
MM-211B	19.568	16.046	42.302	3.2	5.3
AC-4A	19.03	15.85	43.83	3.2	6.6
AC-4B	21.39	16.39	44.62	3.2	5.2
AC-4D	20.91	16.25	44.54	3.2	5.4
AC-4E	20.72	16.35	45.03	3.2	5.8
AC-4J-1	20.76	16.32	46.72	3.2	6.5
AC-4J-2	19.75	16.13	37.97	3.2	2.9
MM-212A	25.099	16.831	45.312	2.8	3.8
MM-212B	25.288	16.954	46.151	2.8	4.0
AC-4H-1	26.05	16.99	45.38	2.8	3.5
AC-4H-2	26.16	17.04	45.14	2.8	3.4
PE DE SERRA GRANITE					
MM-30A	18.161	15.741	37.305	2.55	3.1
MM-30C	18.791	15.908	38.131	2.55	3.3
MM-30D	18.761	15.968	38.06	2.55	3.3
MM-30E	19.629	16.028	38.824	2.55	3.3
MM-31	18.592	15.873	37.801	2.55	3.3
MM-32A	20.774	16.259	40.127	2.55	3.4
MM-32B	22.489	16.545	42.085	2.55	3.6
MM-160A	22.69	16.541	42.368	2.55	3.6
MM-160B	20.629	16.217	40.274	2.55	3.6
MM-160C	20.845	16.279	40.461	2.55	3.6
MM-132	23.361	16.348	39.582		
MM-163	28.738	17.132	52.288		
MM-163bis	28.44	17.074	51.763		

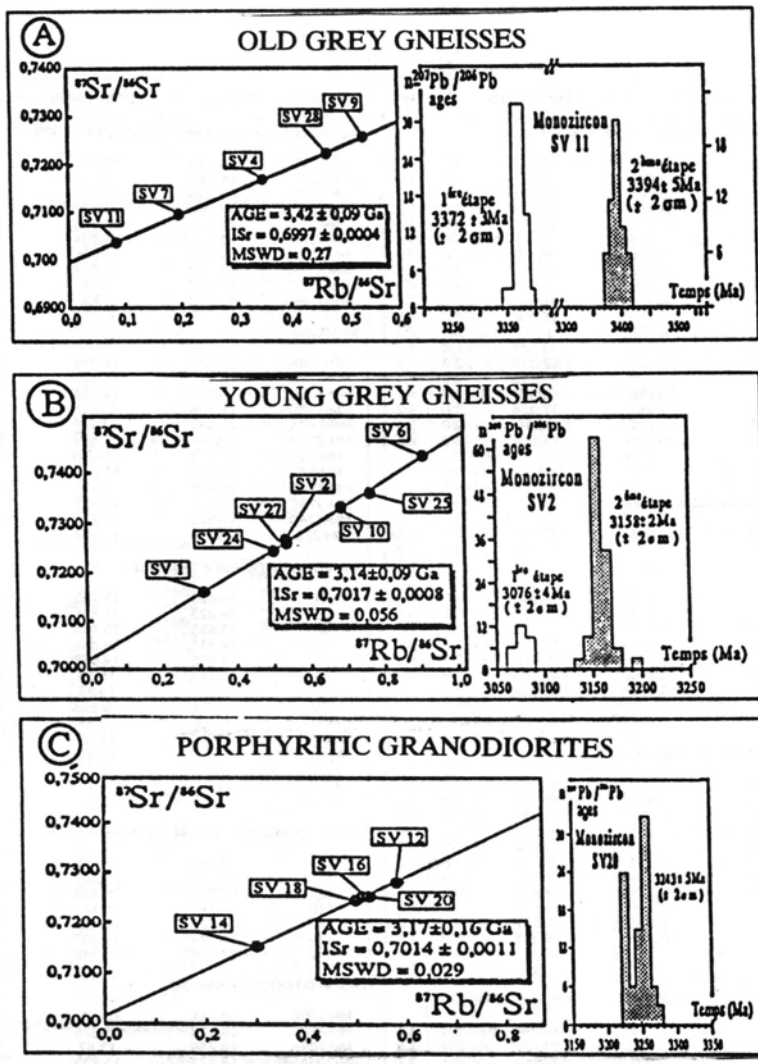

Figure IV.9 - Rb-Sr diagrams and single zircon $^{207}Pb/^{204}Pb$ data for: (A) old grey gneisses; (B) young grey gneisses; (C) porphyritic granodiorites (Martin et al., 1991).

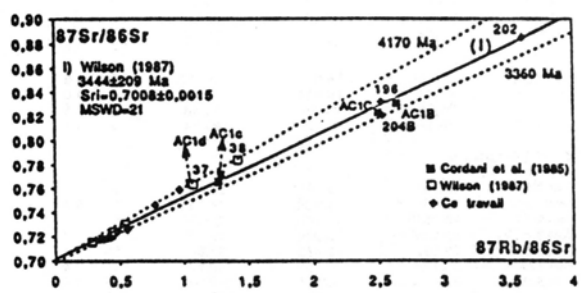

Figure IV.10 - Rb-Sr (whole rock) diagram for the Boa Vista/Mata Verde granitoid. Also displayed are the 4170 and 3360 Ma reference lines that bound the dispersion envelope (Wilson, 1987 and Marinho, 1991).

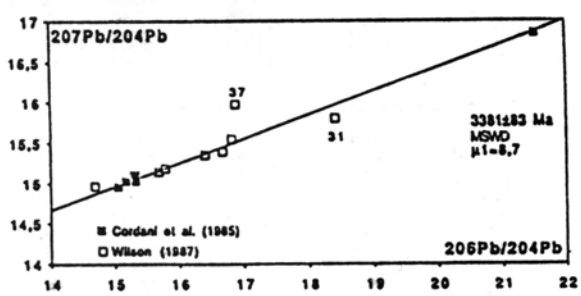

Figure IV.11 - $^{207}Pb/^{204}Pb$ vs. $^{206}Pb/^{204}Pb$ (whole rock) diagram for the Boa Vista/Mata Verde granitoid (Wilson, 1987).

Table IV.4 - Sm-Nd data from Contendas-Mirante belt.

UNIT	SAMPLE	Sm(ppm)	Nd(ppm)	147Sm/144Nd	143Nd/144Nd	ENd(o)	ENd(t)	Tchur(Ga)	TDm(Ga)	ENd(o)Dm	t(AE)
1	MM-209A	9.76	57.07	0.1034	0.510489	-41.92	-3.83	3.482	3.560	8.75	3.200
	MM-210B	10.94	73.50	0.0900	0.510342	-44.79	-1.2	3.254	3.354	8.75	3.200
	MM-211A	10.49	67.65	0.0937	0.510385	-43.95	-1.91	3.310	3.405	8.75	3.200
2	42E	10.8	52.6	0.1242	0.511118	-29.65	0.88	3.173	3.327	8.75	3.300
	42G	11.1	53.5	0.1254	0.511079	-30.41	-0.39	3.307	3.437	8.75	3.300
3	MM-200B	3.92	20.60	0.1152	0.511301	-26.08	-5.28	2.488	2.747	8.75	2.000
	MM-205A	4.26	23.86	0.1079	0.511390	-24.34	-1.69	2.134	2.433	8.75	2.000
	MM-206B	0.59	2.95	0.1202	0.511562	-20.99	-1.47	2.136	2.473	8.75	2.000
4	MM-35	2.87	11.36	0.1526	0.511746	-17.4	-3.34	3.063	3.319	8.75	2.500
	MM-224C	1.50	5.66	0.1606	0.511848	-15.41	-3.89	3.310	3.526	8.75	2.500
	MM-228	2.83	11.67	0.1464	0.511504	-22.12	-6.08	3.409	3.554	8.75	2.500
5	MM-213C	1.40	6.14	0.1375	0.511546	-21.3	1.38	2.793	3.059	8.75	3.000
	MM-213E	1.15	5.30	0.1314	0.511442	-23.33	1.67	2.775	3.025	8.75	3.000
	MM-230B	1.33	6.21	0.1298	0.511391	-24.33	1.29	2.824	3.059	8.75	3.000
	MM-230E	1.33	6.47	0.1243	0.511372	-24.7	3.02	2.650	2.905	8.75	3.000
	MM-230D	2.40	11.90	0.1219	0.511213	-27.8	0.84	2.885	3.089	8.75	3.000
6	MM-1A	3.85	20.11	0.1157	0.511526	-21.69	4.16	2.084	2.414	8.75	2.500
	MM-67	4.08	23.45	0.1052	0.511189	-28.27	0.94	2.401	2.650	8.75	2.500
	MM-72	4.70	23.48	0.1211	0.511529	-21.63	2.47	2.228	2.552	8.75	2.500
	MM-79	4.53	23.80	0.1149	0.511231	-27.45	-1.36	2.609	2.846	8.75	2.500
	MM-145	6.23	32.73	0.1151	0.511451	-23.15	2.89	2.207	2.515	8.75	2.500
	MM-157A	4.00	21.15	0.1143	0.511427	-23.62	2.67	2.230	2.531	8.75	2.500
7	MM-25A	6.31	27.53	0.1385	0.511363	-24.87	-6.3	3.314	3.465	8.75	2.500
	MM-39	3.40	14.77	0.1392	0.511440	-23.37	-5.03	3.153	3.343	8.75	2.500
	MM-151C	2.76	11.69	0.1428	0.511526	-21.69	-4.5	3.122	3.329	8.75	2.500
	MM-152C	4.58	20.31	0.1363	0.511556	-21.11	-1.84	2.715	2.994	8.75	2.500
	MM-158B	5.62	25.51	0.1332	0.511267	-26.74	-6.49	3.266	3.418	8.75	2.500
	MM-98	8.45	44.42	0.1151	0.510975	-32.44	-6.41	3.085	3.240	8.75	2.500
8	MM-40	3.45	14.76	0.1413	0.511703	-18.24	2.97	2.559	2.894	8.75	3.000
	MM-68	3.59	16.45	0.1321	0.511540	-21.42	3.31	2.577	2.871	8.75	3.000
	MM-68bis	3.81	17.40	0.1323	0.511517	-21.87	2.79	2.639	2.920	8.75	3.000
	MM-8	5.95	28.38	0.1267	0.511197	-28.11	-1.31	3.116	3.285	8.75	3.000
	MM-9	5.82	27.95	0.1260	0.511207	-27.91	-0.83	3.062	3.241	8.75	3.000
	MM-15	5.23	23.94	0.1319	0.511367	-24.79	0.01	2.970	3.181	8.75	3.000
	MM-17	5.86	29.13	0.1216	0.511269	-26.71	2.04	2.762	2.988	8.75	3.000
	MM-20	6.60	32.27	0.1237	0.511136	-29.3	-1.37	3.115	3.280	8.75	3.000
	MM-21	4.41	15.38	0.1732	0.511599	-20.27	-11.27			8.75	3.000
	MM-22C	4.68	20.85	0.1356	0.511363	-24.87	-1.48	3.158	3.338	8.75	3.000
	MM-23	7.01	28.38	0.1493	0.511622	-19.82	-1.67			8.75	3.000
	MM-100B	8.47	2.06	0.1469	0.511632	-19.62	-0.54	3.055	3.291	8.75	3.000
9	MM-99D	0.86	3.15	0.1646	0.511612	-20.01	-12.22			8.75	1.900
	MM-99H	0.48	1.52	0.1927	0.512039	-11.68	-10.71			8.75	1.900
	MM-99I	1.72	4.06	0.2561	0.513135	9.69	-4.71			8.75	1.900
	11217	0.55	2.02	0.1646	0.511914	-14.12	-6.34			8.75	1.900
10	MM-95	4.80	32.34	0.0896	0.510730	-37.22	-10.58	2.701	2.877	8.75	1.950
	MM-92	4.08	28.12	0.0877	0.510779	-36.26	-9.15	2.586	2.775	8.75	1.950
	11218	4.10	27.20	0.0911	0.510869	-34.51	-8.24	2.541	2.742	8.75	1.950
11	MM-132	23.24	110.83	0.1267	0.511300	-26.1	-3.34	2.897	3.109	8.75	2.550
	MM-160B	11.89	58.21	0.1234	0.511192	-28.21	-4.37	2.988	3.176	8.75	2.550
	MM-30A	9.70	47.35	0.1238	0.511226	-27.54	-3.84	2.935	3.134	8.75	2.550
	11219	12.8	64.10	0.1207	0.511170	-28.64	-3.91	2.926	3.120	8.75	2.550
12	31	4.4	32.0	0.0828	0.510098	-49.55	-0.86	3.372	3.452	8.75	3.350
	32	4.6	31.9	0.0871	0.510155	-48.44	-1.58	3.425	3.500	8.75	3.350
	33	5.4	38.0	0.0866	0.510168	-48.18	-1.12	3.392	3.471	8.75	3.350
	34	7.1	50.1	0.0862	0.510147	-48.59	-1.36	3.409	3.485	8.75	3.350
	35	3.9	28.1	0.0841	0.510124	-49.04	-0.91	3.376	3.456	8.75	3.350
	36	5.5	38.9	0.0847	0.510141	-48.71	-0.83	3.372	3.452	8.75	3.350
	37	10.9	75.3	0.0873	0.510135	-48.83	-2.06	3.459	3.529	8.75	3.350
	38	7.5	50.3	0.0896	0.510475	-42.19	3.59	3.057	3.184	8.75	3.350

1 - Lagoa do Morro granitoid
2 - Barra da Estiva road junction sub-volcanic body
3 - Neosomes within metapelites (middle unit)
4 - Rio Jacaré sill
5 - Banded Iron Formations (lower unit)
6 - Metapelites from the middle unit
7 - Calco-alkaline volcanic rocks (middle unit)
8 - Tholeiitic volcanic rocks (lower unit)
9 - Tranamazonian granite (Riacho das Pedras)
10 - Transamazonian granite (Gameleira)
11 - Pé de Serra granite
12 - Boa Vista/Mata Verde granitoid

chronology was established by Nutman & Cordani (chapter V, in press), who obtained concordant ages of 3353±5 Ma using SHRIMP in zircons of tonalite sample AC-1E.

High apparent μ_1 value (8.7), together with $T_{DM}Nd$ model ages greater than those of U-Pb in zircons along with negative $\epsilon Nd_{(3350\ Ma)}$ values (between -0.8 and -2.1) suggest a certain period of crustal residence for the source material of the Boa Vista/Mata Verde massif.

THE VOLCANO-SEDIMENTARY SEQUENCE

The considerations presented in chapter III show that the volcano-sedimentary sequence is divided into a lower, a middle and an upper unit.

The lower unit

The available isotopic data for the lower unit involves tholeiitic volcanic rocks, banded iron formations, and the Barra da Estiva road junction rhyolitic sub-volcanic body. The data relative to this rhyolitic body will be discussed first due to their importance for the understanding of the geochronologic evolution of the region.

Barra da Estiva Road Junction Sub-Volcanic Body

At first, it is interesting to review the data of Wilson (1987):

. Rb-Sr errorchron (Fig. IV.12) of sixteen samples (age = 2140±153 Ma; Sr_i = 0.7457±0.0052; MSWD = 3.4);

. Pb-Pb errorchron (Fig. IV.13) of eleven samples (age = 3011±159 Ma; apparent μ_1 = 9.21; MSWD = 25);

. $T_{DM}Nd$ model-ages of 3330 and 3440 Ma (Table IV.4) and $\epsilon Nd_{(3300\ Ma)}$ of -0.4 and -0.9.

This data lead Wilson to interpret the Pb-Pb values (ca 3.0 Ga) as the time of intrusion, those of Rb-Sr (ca 2.1 Ga) as the metamorphic age, and the $T_{DM}Nd$ model age values as the time of extraction from the mantle.

Looking for complementary information, Marinho (1991) determined a zircon U-Pb age by the conventional method. The analyses of five fractions (Table IV.5) define a discordia (MSWD = 2.07) with a lower intersection at 604 + 312/-318 Ma and an upper intersection at 3304 + 31/-24 Ma (Fig. IV.14). This value is higher than that given by the Pb-Pb isochron, but close to that of the $T_{DM}Nd$ model ages. Does it represent the time of intrusion of the rhyolitic body or does it reflect an ancient crustal memory?

In an attempt to find an answer to this question, Marinho (1991) carried out a research on the typology (Pupin, 1980) of the rhyolite zircons. This showed that these zircons have the 100 prism better developed than the 110 prism (100 >> 110), which sometimes is not even present. The 101 pyramid is more developed than 211 (101 >> 211). On Pupin's classification, these zircons belong to types S_{24}, S_{25}, P_5, J_4, J_5

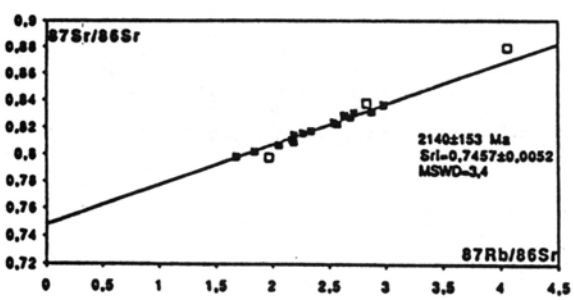

Figure IV.12 - Rb-Sr (whole rock) diagram for the Barra da Estiva road junction sub-volcanic body (Wilson, 1987).

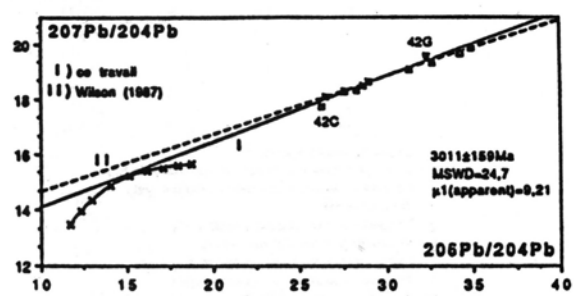

Figure IV.13 - $^{207}Pb/^{204}Pb$ vs. $^{206}Pb/^{204}Pb$ (whole rock) diagram for the Barra da Estiva road junction sub-volcanic body (Wilson, 1987).

Table IV.5 - U-Pb zircon data from Barra da Estiva road junction sub-volcanic body.

		CONCENTRATIONS (ppm)			ATOMIC RATIOS				AGES (Ma)		
Fraction (micrometre) (*1)	Weigh (mg)	U (*2)	Pb Radiog. (*2)	Pb common (*3)	206Pb/204Pb (*4)	206Pb/238U	207Pb/235U	207Pb/206Pb (*5)	206Pb/238U	207Pb/235U	207Pb/206Pb
60-80	3.05	146	100	0.346	12084	0.5612	20.187	0.26088	2872	3100	3256
80-100	0.89	144	97	0.766	5300	0.5536	19.981	0.26179	2840	3090	3258
100-120	1.54	141	96	0.986	4088	0.5588	20.204	0.26224	2862	3101	3260
120-150	2.5	124	83	0.373	9248	0.5464	19.816	0.26305	2810	3082	3265
>150	2.4	141	101	0.315	13357	0.5858	21.409	0.26506	2972	3157	3277

(*1) Non magnetic fractions in isodynamic FRANTZ separetor set at 1.8 ampere, slope o°
(*2) Estimated concentrations (±0.5%)
(*3) Concentration in common lead corrected for contaminating lead
(*4) Measured ratios
(*5) Estimated errors (0.2%)

and D of high temperature (850°C), and are characteristic of volcanic rocks.

This zircon typology, the absence of overgrowths, and the near concordant position of the U-Pb data suggest that the age of ca. 3.3 Ga is near the emplacement of the sub-volcanic body. However, it must be emphasized that this body intrudes tholeiitic volcanic rocks with BIF intercalations. The age of these rocks should then record a maximum limit for its emplacement. As it is seen below, these ages are not always consistent with the U-Pb data of zircons from the sub-volcanic body.

Tholeiitic Volcanic Rocks

The following results are presented by Marinho (1991) for the tholeiitic rocks:

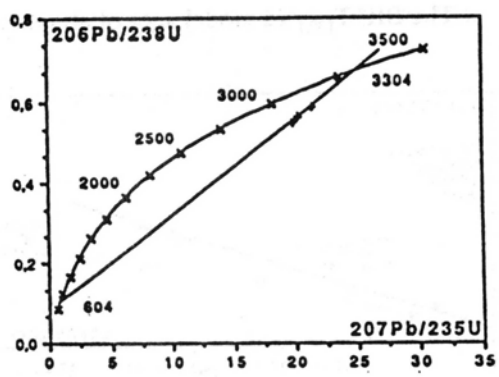

Figure IV.14 - U-Pb concordia diagram for the Barra da Estiva road junction sub-volcanic body (Marinho, 1991).

. scattered data on the $^{207}Pb/^{204}Pb$ vs. $^{206}Pb/^{204}Pb$ (Fig. IV.15);

. $T_{DM}Nd$ model ages grouped in two classes (Table IV.4) with average values close to 2300-3000 Ma (samples 6c, 16, 17, 40) and 3300 Ma (samples 8, 9, 15, 20, 22c and 23). The $\epsilon Nd_{(3000\ Ma)}$ values range between 2.0 and 3.3 and between 0 and -1.7 for the first and second group, respectively;

. scattered data on $^{143}Nd/^{144}Nd$ vs $^{147}Sm/^{144}Nd$ diagram.

Before discussing these data, it is interesting to consider the Zr and Nb behaviour of these tholeiitic rocks. The Zr/Nb vs Zr diagram (Fig. IV.16) indicates two evolutive trends:

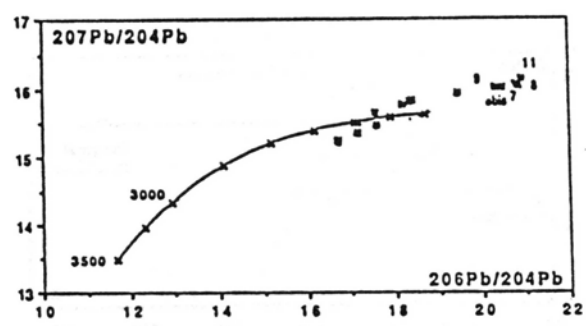

Figure IV.15 - $^{207}Pb/^{204}Pb$ vs. $^{206}Pb/^{204}Pb$ (whole rock) diagram for the tholeiitic volcanic rocks of the Contendas-Mirante belt lower unit (Marinho, 1991).

. one marked by the change in the ratio Zr/Nb proportional to the Zr abundance variation; and

. other characterized by a change in Zr while the Zr/Nb ratio remains constant.

The presence of these two trends might reflect a fractional crystalization mechanism associated to variable rates of partial melting from the same source material, according to the model proposed by Treuil & Varet (1973). Such a process, however, could not respond for the strong growth in ϵNd. Thus, it seems that the evolution took place in the opposite direction, with increases in Zr/Nb ratios reflecting higher degrees of crustal contamination. This contamination is reflected in the decrease of the ϵNd that changes from (+2)-(+3) in samples 6B, 17 and 40 to (0)-(-1.7) in samples 8, 9, 15, 20, 22C and 23.

Marinho (1991) considered the evolution of Nd in samples 6B, 6B (bis), 17 and 40 as rather significant for establishing an age of 3000 Ma as the maximum limit for the time of extraction of these tholeiitic magmas from the mantle. His reasoning was based on the fact that the ϵNd of these samples, when projected beyond 3000 Ma (e.g. 3300 Ma: age of the zircons of the subvolcanic body), acquires values between +5 and +6. Such values are higher than those of the depleted mantle for that time, which, according to Smith & Ludden (1989), should be close to +2. However, ϵNd values in the order of +5 are recorded for 3500 Ma depleted mantle tholeiites (Shirey & Hanson, 1986). Therefore, Nd evolution does not seem to be a sound basis for limiting at 3000 Ma the time of extraction of the tholeiitic liquids from the mantle.

Attempts at determining the ages through isochronic methods proved unfruitful both for Sm-Nd and Pb-Pb. In the latter case, the $^{207}Pb/^{204}Pb$ vs. $^{206}Pb/^{204}Pb$ diagram (Fig. IV.15) shows that, in spite of the scattering, the general disposition of the points do not deviate much from a two-stage evolution model.

Banded Iron Formations (BIF)

The data available are those from Marinho (1991):

. alignment of eleven samples on the $^{207}Pb/^{204}Pb$ vs $^{206}Pb/^{204}Pb$ diagram (Fig. IV.17), with an age of 3265±51 (apparent μ_1 = 9.2 and MSWD = 5.6);

. T_{DM}Nd model ages around 3000 Ma and $\epsilon Nd_{(3000\ Ma)}$ between 0.8 and 3.1 (Table IV.4).

These ϵNd values close to those of DM suggest a predominating mantle influence in the source of these rocks. On the other hand, the position of the points above the normal curve of crust evolution for terrestrial lead shows a model in more than two stages, suggestting a source compatible with the upper crust.

The BIF T_{DM}Nd model ages of about 3000

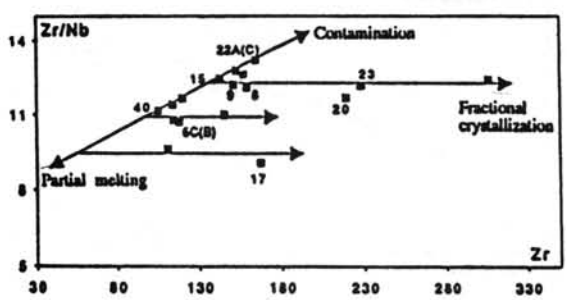

Figure IV.16 - Zr/Nb vs. Zr diagram for tholeiitic volcanic rocks from the Contendas-Mirante belt lower unit (Marinho, 1991).

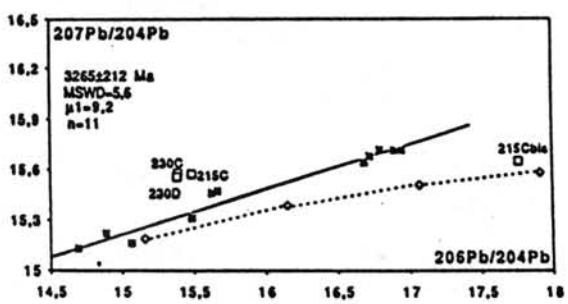

Figure IV.17 - $^{207}Pb/^{204}Pb$ vs. $^{206}Pb/^{204}Pb$ (whole rock) diagram for the banded iron formations of the Contendas-Mirante belt lower unit (Marinho, 1991).

Ma conflict with the zircon U-Pb age (3300 Ma) of the sub-volcanic rhyolitic body.

The Age Problem of The Lower Unit

It is clear that from the age values produced by the different methods used, a certain ambiguity still persists regarding the age relationships between the tholeiites, the banded iron formations and the Barra da Estiva road junction sub-volcanic rhyolite. In spite of that, we believe that the zircon U-Pb ages of the subvolcanic body (3.3 Ga), very close to concordia, best represents the age of formation of all these lithologies.

The middle unit

The studies about the isotopic signature of this sequence were carried out by Marinho (1991). They included metapelites and associated neosomes from the Rio Gavião and Mirante formations as well as calc-alkaline volcanic rocks interbedded in the last one.

Metapelites of The Rio Gavião and Mirante Formations

These two formations consist in fact of one lithological sequence metamorphosed under different grades (see Chapter III).

The following isotopic results were obtained by Marinho:

. T_{DM}Nd model ages of six samples between 2420 and 2850 Ma (three samples at 2500 Ma) and $\epsilon Nd_{(2500\ Ma)}$ between -1.4 and +4.2 (Table IV.4).

The T_{DM}Nd ages close to 2500 Ma, that represent the lower limit for the metapelite sedimentation time, coincide, within the experimental error, with Pb-Pb ages obtained for the interbedded calc-alkaline volcanic rocks, as shown further on. The ϵNd values of the metapelites indicate a very short time of crustal residence for its source material.

Neosomes within the Metapelites

As the origin of these neosomes is connected to the regional metamorphism of the volcano-sedimentary sequence, they were used by Marinho (1991) to date this metamorphic event. The following results were obtained:

. Rb-Sr isochorn (Fig. IV.18) of eight samples (age = 2012±17; Sr_i = 0.70321±0.00017; MSWD = 1.17);

. T_{DM}Nd model ages of three samples: 2435, 2475 and 2750 Ma.

The Rb-Sr isochronic age of 2012 Ma dates the metamorphism that produced the zoneography displayed by the volcano-sedimentary sequence (Chapter III). This metamorphism is connected to the Transamazonian event.

The very low Sr_i ratios are compatible with a mantle source or a crustal source of very short residence time. This is in agreement with the data presented above for the metapelites of the Rio Gavião and Mirante formations.

Calc-Alkaline Volcanic Rocks

As already stated, these lithologies are centimetric to metric intercalations within the Mirante Formation metapelites. Their isotopic signature is characterized (Marinho, 1991) by two approximately parallel alignments of three and seven samples in the $^{207}Pb/^{204}Pb$ vs. $^{206}Pb/^{204}Pb$ diagram (Fig. IV.9) the regressions of which give respectively:

. age = 2490±81 Ma; apparent μ_1 = 8.8; MSWD = 1.1

. age = 2519±16 Ma; apparent μ_1 = 8.2; MSWD = 1.2.

. T_{DM}Nd model ages between 3250 and 3450Ma except for one sample of 3000 Ma; the $\epsilon Nd_{(2500\ Ma)}$ of this sample is 1.8, while for the others it falls between -4.5 and -6.5 (Table IV.4).

Before discussing these data, we must

stress the existence of a large dispersion in the Zr/Nb ratio among the different samples of these calc-alkaline rocks, reflecting heterogeneity either inside the source or acquired along their evolution.

The existence of two alignments in the $^{207}Pb/^{204}Pb$ vs. $^{206}Pb/^{204}Pb$ may be questioned. However, if we consider the whole data points as a scattered trend, the age obtained by regression of all points is of the same order (line I, Fig. IV.19) as those from the two alignments. Furthermore, the invariability of the Th/U ratio (close to 3 - see $^{208}Pb/^{204}Pb$ vs. $^{206}Pb/^{204}Pb$ diagram of Fig. IV.20) is compatible with a normal magmatic process and attests the closed nature of the system since the extrusion time. Thus, the two alignments appear to exist and should be attributed to source heterogeneity.

The position of both alignments above the normal evolution curve for terrestrial Pb denotes an isotopic three-stage development. This feature and the highly radiogenic composition of the lead suggest a source in the upper continental crust. The crustal origin is also indicated by the negative values of the ϵNd_T (Table IV.4). This evolution is compatible with a source within the lower sequence as shown in Fig. IV.21.

Thus, these isotopic data indicate an age of about 2500 Ma for the extrusion time of these calc-alkaline rocks. This age coincides, within the experimental error, with the value of the $T_{DM}Nd$ model ages for the lower limit of sedimentation of the metapelites.

The upper unit

As stated previously, this unit is represented by meta-arkoses with conglomeratic beds of the Areião formation.

The only available isotopic data are the U-Th-Pb zircon ion microprobe determinations made by Nutman et al. (in press). These determinations were performed in detritic zircons of a conglomeratic bed that occurs as a tectonic slice within the metapelites of the middle unit. The data obtained from these zircons gave U-Pb concordant ages between 2710 and 2150 Ma (Chapter V).

These data defines the deposition time of the conglomerate between 2150 and 1900 Ma, the ages of the youngest detrital zircons and of the granitic Transamazonian intrusions that crosscut the upper sequence, respectively. This shows a discontinuity relatively to the middle unit, the age of which is around 2500 Ma, as shown previously.

THE INTRUSIVE ROCKS

In this section we will deal with the following plutons:

. The Lagoa do Morro granitoid (*sensu lato*)

. The Pé de Serra granite;

. The Rio Jacaré sill; and

. The Transamazonian granites.

The Lagoa Do Morro Granitoid (s.l.)

Before presenting the isotopic data of this pluton, it must be remembered (chapter III) that Marinho (1991) identified within the previously named Lagoa do Morro granitoid (Marinho et al., 1980; Marinho & Sabaté 1982; Cordani et al., 1985) three independent bodies with distinct petrographic and geochemical features. These bodies were then named "Serra dos Pombos granitoid", "Anagé/Pau de Colher granitoid" and "Lagoa do Morro granitoid (*sensu stricto*)".

The isotopic results available are the following (filled symbols = Marinho, 1991; open symbols = Cordani et al., 1985):

. Rb-Sr errorchron (Fig. IV.22) of seven samples (age = 2844±114 Ma; Sr_i = 0.7041±0.0020; MSWD = 7.9);

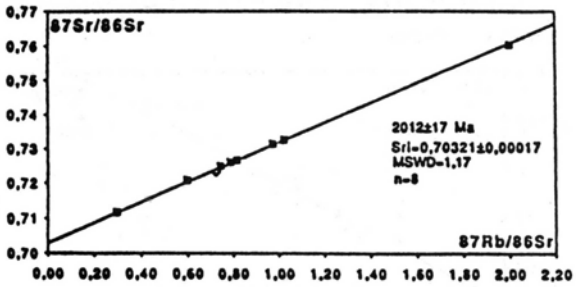

Figure IV.18 - Rb-Sr (whole rock) diagram for neosome within metapelites from the Contendas-Mirante belt middle unit (Marinho, 1991).

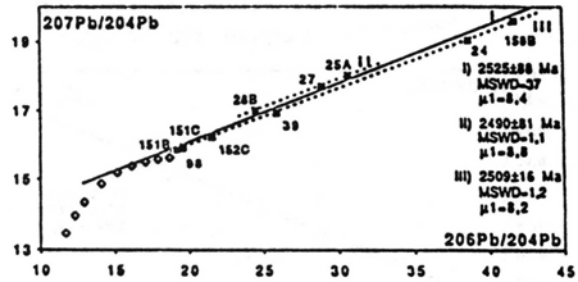

Figure IV.19 - $^{207}Pb/^{204}Pb$ vs. $^{206}Pb/^{204}Pb$ (whole rock) diagram for calc-alkaline volcanic rocks from the Contendas-Mirante belt middle unit (Marinho, 1991).

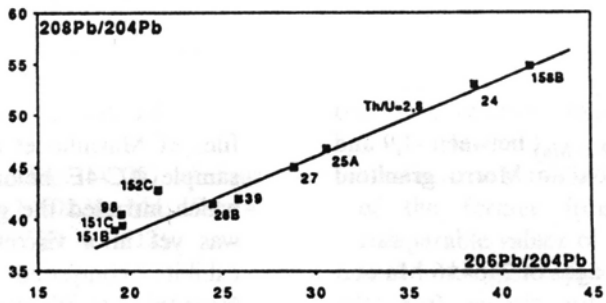

Figure IV.20 - $^{208}Pb/^{204}Pb$ vs. $^{206}Pb/^{204}Pb$ (whole rock) diagram for calc-alkaline volcanic rocks from the Contendas-Mirante belt middle unit (Marinho, 1991).

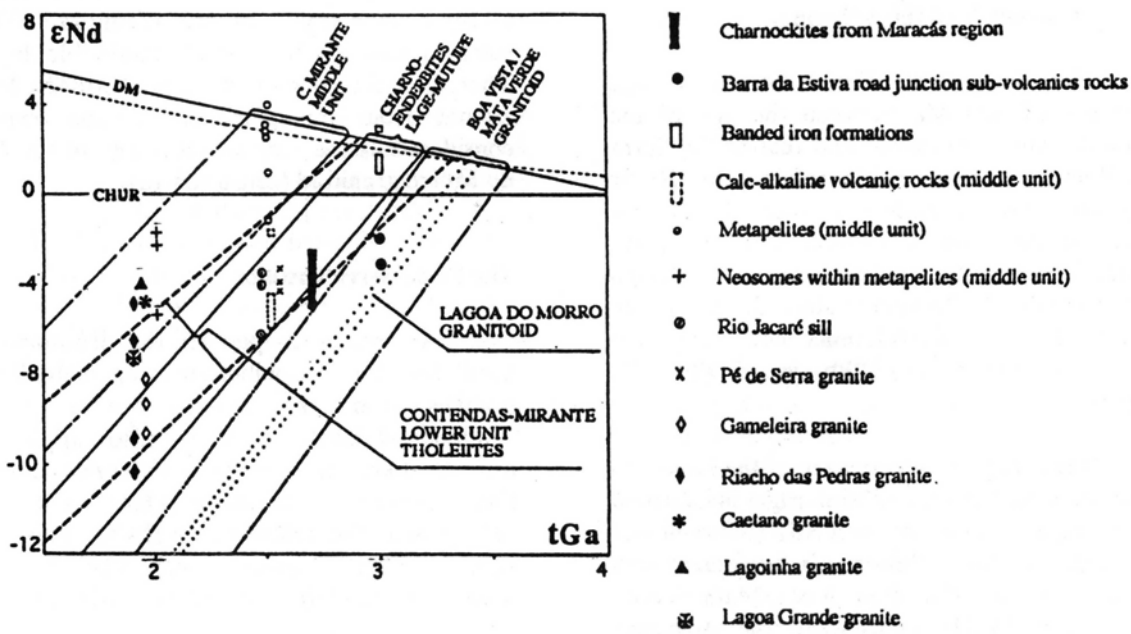

Figure IV.21 - Nd isotope evolution of the area in relation to time (Marinho, 1991).

. scattered data on the $^{207}Pb/^{204}Pb$ vs. $^{206}Pb/^{204}Pb$ diagram (Fig. IV.23);

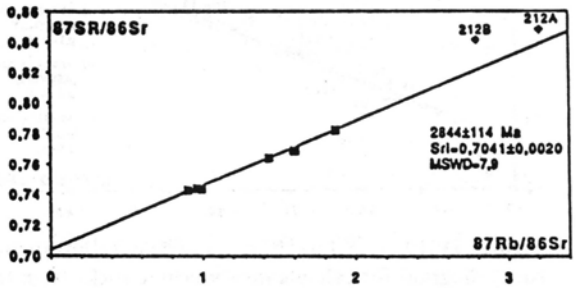

Figure IV.22 - Rb-Sr (whole rock) diagram for Lagoa do Morro (■) and Serra dos Pombos (♦) granitoids (Marinho, 1991).

. $T_{DM}Nd$ model ages between 3360 and 3560 Ma; $\epsilon Nd_{(3200\ Ma)}$ between -1,9 and -3,8 for the Lagoa do Morro granitoid (*s.s.*).

. U-Pb concordant ages of 3184±6 Ma and about 2850 Ma for zircons from the Lagoa do Morro (sample AC-4E) and the Serra dos Pombos (sample AC-4G) massifs, respectively. These determinations made by Nutman & Cordani (in press), are discussed in Chapter V of this volume.

The data about zircons stress an age difference of 400 Ma between the age of the Lagoa do Morro granitoid and that of the Serra dos Pombos granitoid. Therefore, the Rb-Sr errorchron should reflect a resetting of this system at the time of formation of the latter massif. This resetting would also have affected the whole-rock U-Pb system since the points are close to the 2800 Ma reference line despite the scatter on the $^{207}Pb/^{204}Pb$ vs. $^{206}Pb/^{204}Pb$ diagram.

Regarding the provenance of the Lagoa do Morro granitoid (*s.s.*), a crustal origin is indicated by the negative values of the ϵNd_T (between -1.9 and -3.8). This Nd evolution is in agreement with a source within the Boa Vista/Mata Verde granite (Fig. IV.21). Conversely, the strontium initial ratio of 0.706 at 2844 Ma becomes 0.700 at 3200 Ma (average $^{87}Rb/^{86}Sr$ = 1.34), indicating a mantle source.

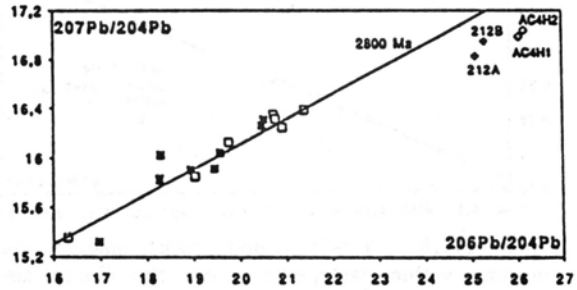

Figure IV.23 - $^{207}Pb/^{204}Pb$ vs. $^{206}Pb/^{204}Pb$ (whole rock) diagram for Lagoa do Morro (squares) and Serra dos Pombos (diamonds) granitoids. Filled symbols, after Marinho (1991); open symbols, after Cordani (1985).

Recent review of the sampling recording files of Marinho et al. (1980) has revealed that sample AC-4E belongs to a granodioritic dike which intruded the granitoid while this last one was yet in a viscous state. The granodiorite exhibits composed rheologic features, from Newtonian to Bingham conditions, in relation to the granitoid, with a pseudoplastic predominating condition where the contacts are either sharp or extremely irregular (fractal). The granodiorite occurs either as enclaves in the granitoid or with enclaves of granitoid mush, locally with unstable feldspar phenocrysts of the granitoid. These features characterize coeval immiscible liquids. Therefore, the concordant ages of 3184±6 Ma in zircons from the granodioritic dike can be considered as the emplacement age of the Lago do Morro granitoid (sensu strictu).

The Pé de Serra Granite

As seen in Chapter III, this denomination, used for the amphibole-bearing sub-alkaline granites from the eastern border of the Contendas-Mirante belt, is also applied to associated alkaline granites and syenites, although their genetic relationships have not been determined. The following results for these sub-alkaline (filled squares) and alkaline (open squares) rocks were obtained by Marinho (1991):

Sub-alkaline rocks:

. Pb-Pb errorchron (Fig. IV.24) of ten samples (age = 2559±110 Ma; apparent μ_1 = 8.5; MSWD = 8.7)

. Rb-Sr scattered data between reference lines of 2550 and 2200 Ma on the $^{87}Sr/^{86}Sr$ vs. $^{87}Rb/^{86}Sr$ diagram (Fig. IV.25);

. $T_{DM}Nd$ model ages of three samples, of 3120, 3135 and 3175 Ma and $\epsilon Nd_{(2550\ Ma)}$ of -3.9, -3.8 and -4.4.

Alkaline rocks:

. Pb-Pb isochron (Fig. IV.24) of three samples (age = 2282±81 Ma; apparent μ_1 = 8.1; MSWD = 0.22);

. Rb-Sr errorchron (Fig. IV.25) of four samples (age = 1250±36 Ma; Sr_i = 0.74412±0.0006; MSWD = 10.12);

. $T_{DM}Nd$ model age of 3110 Ma (one sample).

Notwithstanding the low number of samples available for the alkaline rocks, it seems that their isotopic behaviour is distinct from that of the sub-alkaline rocks.

In the sub alkaline rocks the constancy of the Th/U ratio at about 3.7 (Fig. IV.26) is in agreement with a normal magmatic process, denoting a closed behaviour of the U-Th-Pb system since the intrusion of these rocks. Thus, the 2550 Ma age, obtained from the $^{207}Pb/^{204}Pb$ vs. $^{206}Pb/^{204}Pb$ diagram, must represent the time of intrusion. The point scattering on the $^{87}Sr/^{86}Sr$ vs. $^{87}Rb/^{86}Sr$ diagram suggests a resetting of the Rb-Sr system.

Regarding the origin of these sub alkaline rocks, the position of the Pb-Pb errorchron above the normal evolution curve for terrestrial lead indicates development in at least three stages, which is in agreement with the crustal origin shown by the negative ϵNd_T values. The Nd evolution (Fig. IV.21) is compatible with a source within the charno-enderbitic rocks from the Lage-Mutuípe region.

The marked discrepancy in the ages of the alkaline rocks (2280 Ma obtained by the Pb-Pb isochron and 1250 Ma by the Rb-Sr errorchron) may bear no geologic significance, resulting only from the very small number of samples analysed. Alternatively, however, one can suppose that the Pb-Pb age represents the time of "formation" of these alkaline rocks and that the 1250 Ma age corresponds to the isotopic homogeneization of the Rb-Sr system in the mid-proterozoic Espinhaço Cycle. Ages as low as these have been reported (Cordani et al., 1985) for tholeiitic volcanic rocks from the lower sequence of the Contendas-Mirante belt in its northwesterm sector.

The similarity of the REE spectra of both alkaline and sub-alkaline rocks suggests an origin of the former from the latter rocks. The comparable values of the $T_{DM}Nd$ model ages for both lithologies support this hypothesis.

The Rio Jacaré Sill

The following isotopic data are presented by Marinho (1991) for the lithologies of the mafic/ultramafic sill of the Rio Jacaré:

. Pb-Pb errorchron (Fig. IV.27) of twelve samples (age = 2474±72 Ma; μ_1 = 8.4; MSWD = 3.7);

. $T_{DM}Nd$ model ages between 3320 and 3550 Ma and $\epsilon Nd_{(2500\ Ma)}$ between -3.3 and -6.1 (Table IV.4).

It should be remembered that the Y/Nb and Zr/Nb ratios in the upper and lower zones of the sill evolve according to trends compatible with crustal contamination, which is also reflected by the negative values of the ϵNd_T within the two zones (Fig. IV.28). The decrease in the Nd values from -3.3 to -6.6 associated with the increase of the Y/Nb and Zr/Nb ratios between the samples 35 and 228 of the upper zone reinforces the indication of crustal contamination.

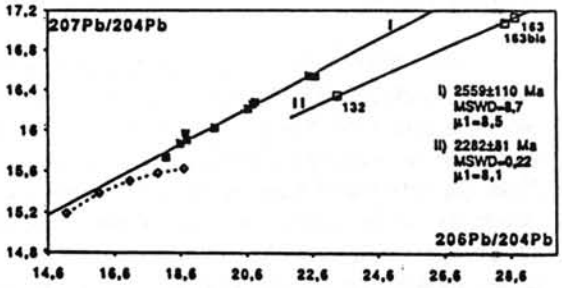

Figure IV.24 - $^{207}Pb/^{204}Pb$ vs. $^{206}Pb/^{204}Pb$ (whole rock) diagram for the Pé de Serra granite. (■) = sub-alkaline rocks; (□) = alkaline rocks (Marinho, 1991).

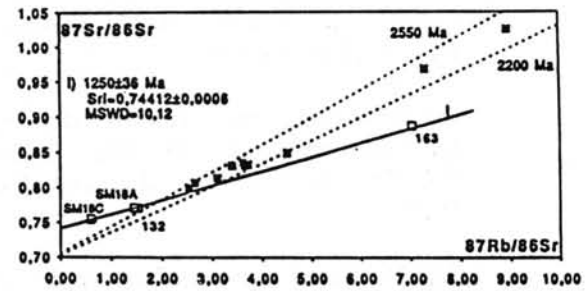

Figure IV.25 - Rb-Sr (whole rock) diagram for the Pé de Serra granite. (■) = sub-alkaline rocks; (□) = alkaline rocks (Marinho, 1991).

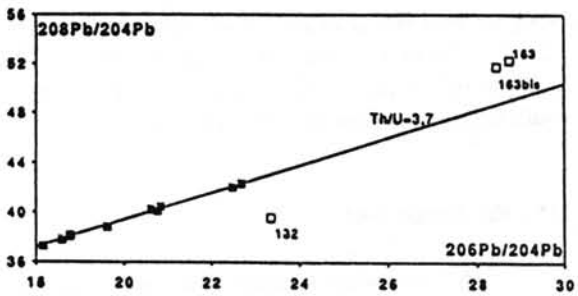

Figure IV.26 - $^{208}Pb/^{204}Pb$ vs. $^{206}Pb/^{204}Pb$ (whole rock) diagram for the Pé de Serra granite. (■) = sub-alkaline rocks; (□) = alkaline rocks (Marinho, 1991).

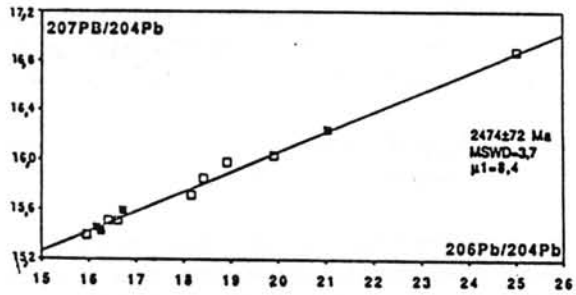

Figure IV.27 - $^{207}Pb/^{204}Pb$ vs. $^{206}Pb/^{204}Pb$ (whole rock) diagram for the Rio Jacaré sill. (■) = lower zone; (□) = upper zone (Marinho, 1991).

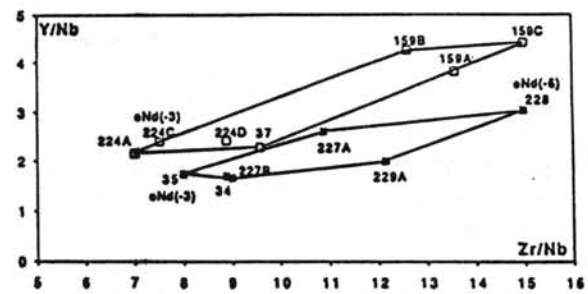

Figure IV.28 - Y/Nb vs. Zr/Nb diagram for the Rio Jacaré sill. (■) = lower zone; (□) = upper zone (Marinho, 1991).

The constancy of the Th/U ratio at about 3.4 (Fig. IV.29) not only reflects the magmatic heritage of these mafic lithologies, but also points to the Pb-Pb age of 2474 Ma as the actual time of their formation. This age is well in accordance with the described presence of xenoliths within the sill of calc-alkaline volcanic rocks from the middle unit of the Contendas-Mirante sequence (Brito, 1984). The $T_{DM}Nd$ model ages are much too high certainly due to the values of the $^{147}Sm/^{144}Nd$ ratios that are equal or higher than 0.15.

The Transamazonian Granites

These granites are part of a major alignment, about 500 km long, of granitoid bodies that occupy the central sector of the São Francisco Craton, between the Contendas-Mirante belt in the south and the Jacobina Group in the north. Here, we will discuss the Gameleira and the Riacho das Pedras massifs, that are examples of late- and post-tectonic types, respectively. The following isotopic data were obtained by Marinho (1991):

Gameleira granite:

. Rb-Sr errorchron (Fig. IV.30) of seven samples (age = 1947±54 Ma; Sr_i = 0.7072±0.0044; MSWD = 3.0);

. $\epsilon Nd_{(1950\ Ma)}$ of three samples of -8.2 and -10.6 (Table IV.4).

Riacho das Pedras Granite:

. Rb-Sr errorchron (Fig. IV.31) of nine samples (age = 1908±13 Ma; Sr_i = 0.746±0.011; MSWD = 1.6);

. $\epsilon Nd_{(1900\ Ma)}$ of four samples of -4.7, -6.3, -10.7 and -12.2 (Table IV.4).

The high strontium initial ratios as well as the strongly negative values of ϵNd_T suggest a crustal origin for these two granitic bodies. For the Gamaleira body, the Nd evolution (Fig. IV.21) is compatible with a source either within the lower unit of the Contendas Mirante sequence or within the charno-enderbitic rocks from Laje-Mutuípe. As for the Riacho das Pedras granite, the possibilities of sources are wider, because, besides those indicated for the Gamaleira massif, its Nd evolution is also compatible with the upper unit of the Contendas-Mirante sequence. As already stated by Sabaté et al. (1990), if one supposes that the thrusting of the Jequié granulitic belt over the Contendas-Mirante belt was previous to or simultaneous with these intrusions, the idea that the Laje-Mutuípe charno-enderbitic rocks are the source of these granites should be discarded.

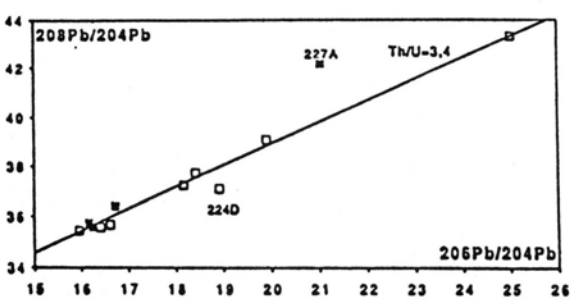

Figure IV.29 - $^{208}Pb/^{204}Pb$ vs. $^{206}Pb/^{204}Pb$ (whole rock) diagram for the Rio Jacaré sill. (■) = lower zone; (□) upper zone (Marinho, 1991).

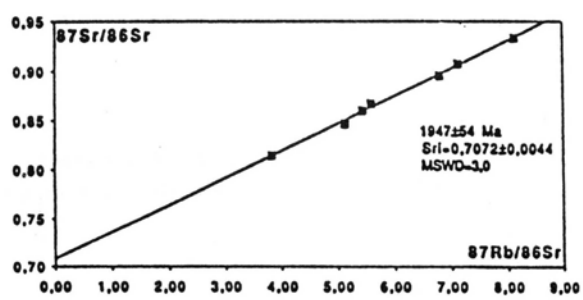

Figure IV.30 - Rb-Sr (whole rock) diagram for the Gameleira granite (Marinho, 1991).

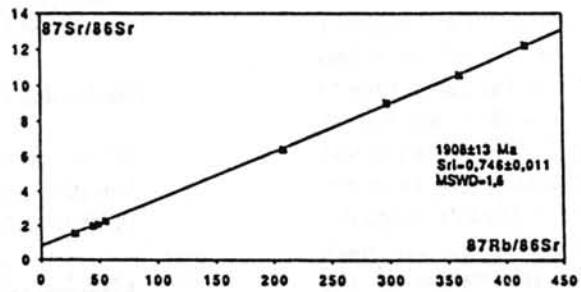

Figure IV-31 - Rb-Sr (whole rock) diagram for the Riacho das Pedras granite (Marinho, 1991).